European Journal of Lipid Science and Technology

WILEY-VCH

European Journal of
Lipid Science and Technology

RESEARCH ARTICLE OPEN ACCESS

Eicosapentaenoic Acid Is Most Oxidatively Stable in the *sn*-2 Position of Triacylglycerols Compared with *sn*-3 and *sn*-1

Annelie Damerau[1] | Eija Ahonen[1] | Maaria Kortesniemi[1] | Haraldur G. Gudmundsson[2] | Baoru Yang[1] | Gudmundur G. Haraldsson[2] | Kaisa M. Linderborg[1]

[1]Food Sciences, Department of Life Technologies, University of Turku, Turku, Finland | [2]Science Institute, University of Iceland, Reykjavik, Iceland

Correspondence: Kaisa M. Linderborg (kaisa.linderborg@utu.fi)

Received: 10 October 2024 | **Revised:** 7 March 2025

Funding: This research was supported by the Research Council of Finland (Grant 315274); Finnish Cultural Foundation; Niemi Foundation.

Keywords: antioxidant | autoxidation | eicosapentaenoic acid (EPA) | omega-3 fatty acid | oxidomics | triacylglycerols (TAG) enantiomers

ABSTRACT

Eicosapentaenoic acid (EPA) is an omega-3 polyunsaturated fatty acid (PUFA), which is easily oxidized based on its high level of unsaturation. So far, it is not fully clear how the location of EPA in triacylglycerols (TAGs) affects its stability. Here, the oxidative stability of EPA in regio- and enantiopure TAGs was investigated for the first time. For analysis of the complete oxidation behavior at 50 °C, headspace solid-phase micro extraction with gas chromatography–mass spectrometry (HS-SPME–GC–MS), liquid chromatography–MS (LC–MS), and nuclear magnetic resonance (NMR) spectroscopy were used, and the data obtained with all used methods was examined in combination using multivariate analysis (oxidomics approach). Oxidation patterns of EPA-containing TAGs were similar as seen previously for docosahexaenoic acid (DHA)-containing ones as shown in the abundance of propanal, 1-penten-3-ol, 2,4-heptadienal, or 5-ethyl-2(5*H*)-furanone. EPA in *sn*-2 was clearly the most stable as seen earlier for neat oil of regiopure TAGs-containing EPA and other omega-3 PUFAs at *sn*-2 position. The stability of EPA in *sn*-1 and *sn*-3 was expected to be identical under the achiral conditions. However, a minor tendency for better stability of *sn*-3 compared with *sn*-1 was seen at certain time points, the difference most likely arising from differences in levels of minor undetected and unidentified prooxidants. *Practical Applications*: On the basis of the results of this study, *sn*-2 should be highly favored for eicosapentaenoic acid in triacylglycerols to improve the stability of neat oils. This is of high interest for enzymatic restructuring processes of eicosapentaenoic acid-rich oils, such as those used for marine oil concentrates. By using enzymes with right regio- and enantiospecificity, the oxidative stability of omega-3 concentrates could be significantly improved over a randomized configuration of fatty acids in triacylglycerols. The findings in this study further contribute to knowledge on the formation of oxidation compounds from eicosapentaenoic acid as not all oxidation compounds reported in this study have been reported earlier. This will contribute to finding new solutions on how to analyze lipid oxidation in the future. Additionally, the reported experimental setup and oxidomic approach could be used to study other lipid species at different temperatures to achieve a complete picture on their oxidative behavior.

Abbreviations: BHT, butylated hydroxytoluene; DHA, docosahexaenoic acid; EPA, eicosapentaenoic acid; 1ET, regio- and enantiopure asymmetrically structured (*S*)-AAB-type *sn*-1 eicosapentaenoic acid-containing triacylglycerols; 2ET, regiopure symmetrically structured ABA-type *sn*-2 eicosapentaenoic acid-containing triacylglycerols; 3ET, regio- and enantiopure asymmetrically structured (*R*)-AAB-type *sn*-3 eicosapentaenoic acid-containing triacylglycerols; FID, flame ionization detector; GC, gas chromatography; HS-SPME, headspace solid-phase micro extraction; HPLC, high-performance liquid chromatography; MS, mass spectrometry; NMR, nuclear magnetic resonance; PCA, principal component analysis; n-3 PUFA, omega-3 polyunsaturated fatty acid; QTOF, quadrupole/time-of-flight; TAGs, triacylglycerols; VSOPs, volatile secondary oxidation products.

[Correction added on May 31 2025, after first Online publication: Copyright line for this article was updated in this version.]

1 | Introduction

Eicosapentaenoic acid (EPA, C20:5), a long-chain *n*-3 polyunsaturated fatty acid (*n*-3 PUFA), is considered an essential compound for human health. EPA increases anti-inflammatory eicosanoids in the human body and plays, therefore, an important role in homeostatic and inflammatory processes, which are linked to numerous diseases, including infection, inflammation, cancer, and cardiovascular diseases. Further, it is vital for growth and development and reduces plasma triglyceridemia [1]. Marine foods are the main dietary sources of EPA in the human diet. In addition, *n*-3 food supplements based on EPA-rich marine oils and foods fortified with marine oil are alternative sources for EPA.

Due to its high level of unsaturation containing five double bonds, EPA oxidizes easily. Formed oxidation products can be absorbed by the human body and are biologically active and toxic [2]. Already mildly oxidized *n*-3 PUFA have been shown not to provide the same health benefits as the non-oxidized ones [3]. Further, lipid oxidation also lowers the sensory quality of food products rich in *n*-3 PUFAs by the formation of unpleasant flavors caused by volatile secondary oxidation products (VSOPs). Therefore, the preventing oxidation of EPA in foods and food supplements during production and storage is of high importance for human health and sensory quality.

One aspect often not considered concerning the oxidative stability of EPA is the effect of molecular lipid structure. EPA is naturally and in food supplements mainly present in triacylglycerols (TAGs). In TAGs, it is either located in the *sn*-1, *sn*-2, or *sn*-3 positions of the glycerol backbone. There are some published studies where the randomization of natural oils or synthetic TAGs has been utilized for examining the influence of structural characteristics of TAGs on the oxidative stability of *n*-3 PUFAs [4–8]. However, they have shown contradictory results. The lack of regio- or stereopure model compounds suitable for these kinds of studies has been the main problem in achieving concise conclusions, as without model compounds, too many factors change simultaneously.

Stability of EPA in regiopure TAG models has only been investigated in two publications [9, 10] and not at all in enantiopure TAG models yet, to the knowledge of the authors. If EPA was together with two saturated FAs in TAGs, the EPA was more stable at the *sn*-2 position than *sn*-1/3 [9]. However, no effect of *sn*-position was found in organic solvent [10] compared to neat oil [9]. Wijesundera et al. [11] and Shen and Wijesundera [12] showed similar findings for regiopure TAG models containing docosahexaenoic acid (DHA, C22:6) in both neat oil and emulsion systems, respectively. DHA was more stable to oxidation when located at the *sn*-2 position in TAGs compared to *sn*-1/3. Our own study [13] included regiopure symmetrically structured ABA-type TAGs and regio- and enantiopure asymmetrically structured AAB-type TAGs and showed highest stability for DHA in *sn*-2 with and without the addition of an antioxidant. Interactions of acyl chains within the same TAG molecule and steric hindrance for hydroperoxide formation could cause differences in the oxidation rate of TAG regioisomers [5, 11, 13]. The stability of DHA in *sn*-1 and *sn*-3 was similar, with slight tendency toward better stability in *sn*-3 without any addition of an antioxidant. With the addition of a common chiral antioxidant, in this case *RRR*-α-tocopherol, higher oxidative stability for *sn*-1 compared to *sn*-3 was seen. This can be explained by diastereomeric interactions between DHA in *sn*-1 position and *RRR*-α-tocopherol, which enhanced the protective effect of *RRR*-α-tocopherol. This was the first oxidation study undertaken with such enantiopure compounds. Both EPA and DHA belong to the *n*-3 fatty acid family, which would suggest similar oxidation behavior for EPA as seen for DHA. However, differences in overall oxidation rate caused by chain length and unsaturation dissimilarities may affect oxidation rates of TAG isomers of these two *n*-3 PUFAs differently.

The hypothesis of this study was that the oxidative stability of EPA is similarly dependent on its location in the glycerol backbone as seen before for DHA. Further, by the addition of an achiral antioxidant, minor differences in the oxidative stability between *sn*-1 and *sn*-3, as seen in DHA, could be heightened in EPA, as the oxidation is slowed down. Should the EPA and DHA behave similarly, more definite conclusions on the oxidation pattern could be drawn. Thus, here we compared the oxidative stability of EPA in TAGs, located either in one of the terminal *sn*-1 or *sn*-3 positions, or in the middle, the *sn*-2 position, in the presence of a minor amount of an achiral antioxidant (in this case butylated hydroxytoluene; [BHT]). Regiopure structured TAGs of the ABA type and regio- and enantiopure TAGs of the AAB type were synthesized and then oxidized under controlled conditions (50 °C in the dark). Oxidation behavior was studied at different time points using modern gas chromatographic (GC) or liquid chromatographic (LC) methods with mass spectrometric (MS) detection and nuclear magnetic resonance (NMR) spectroscopy to allow direct analysis of lipid oxidation compounds at different stages of oxidation. VSOPs were studied with headspace solid-phase micro extraction (HS-SPME) combined with GC–MS. Data of all non-targeted analysis methods were combined and analyzed using principal component analysis (PCA). This oxidomics approach allows simultaneously detection of different classes of oxidation products and thereby the detection of several possible oxidation pathways [14].

2 | Materials and Methods

2.1 | Sample Materials

Regiopure symmetrically structured ABA-type EPA-TAG (*sn*-2; 2ET) and regio- and enantiopure asymmetrically structured (*S*)-AAB (*sn*-1; 1ET) and (*R*)-AAB (*sn*-3; 3ET) EPA-TAGs (Figure 1) synthesized from pure palmitic acid (C16:0; A) and EPA (B) (Larodan, Solna, Sweden) were investigated in the presence of 0.003% (w/w) BHT (≥99% GC-standard from Sigma-Aldrich, Buchs, Switzerland). The synthesis/steps of the synthesis of regiopure and enantiopure EPA-TAGs were described by Halldorsson et al. [15], Kristinsson and Haraldsson [16], Magnusson and Haraldsson [17], Kristinsson et al. [18], and Kalpio et al. [19]. A short summary of synthesis protocol can be found for DHA-TAGs in Damerau et al. [13]. Using ^{1}H and ^{13}C NMR and infrared spectroscopy and accurate MS (HRMS) analyses, the chemical and regioisomeric purity of all products and intermediates was established. The enantiomeric purity of the EPA-TAG enantiomers was analyzed by chiral-phase recycling high-performance LC (HPLC) [19]. All TAG samples were kept under argon for transport and stored at −80 °C until analysis.

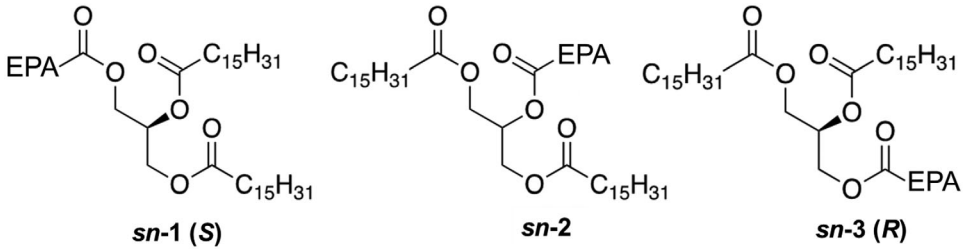

FIGURE 1 | Chemical structure of regio- and enantiopure triacylglycerols with eicosapentaenoic (EPA) and palmitic acid (C16:0).

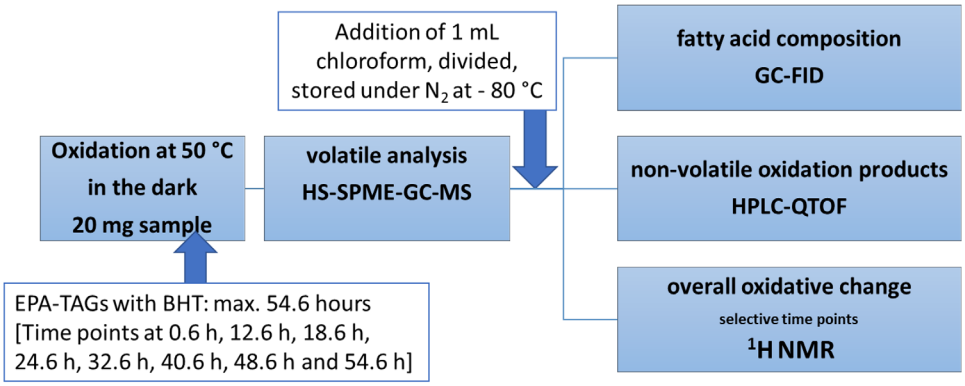

FIGURE 2 | Scheme of experimental setup of oxidation trial of EPA-containing TAGs with BHT; HS-SPME–GC–MS, GC–FID, high-performance liquid chromatographic with a quadrupole/time-of-flight tandem mass spectrometer, ^{1}H NMR spectroscopy. ^{1}H NMR, proton nuclear magnetic resonance; BHT, butylated hydroxytoluene; EPA, eicosapentaenoic acid; GC–FID, gas chromatographic with flame ionization detector; HPLC–QTOF, high-performance liquid chromatographic with a quadrupole/time-of-flight; HS-SPME–GC–MS, headspace solid-phase micro extraction with gas chromatography–mass spectrometry; TAG, triacylglycerol.

2.2 | Experimental Setup for the Oxidation Trial

A similar experimental setup (Figure 2) as in our previous studies [13, 20] was used. The EPA-TAGs 1ET, 2ET, and 3ET were dissolved into *n*-hexane (VWR, Gliwice, Poland), and 0.003% (w/w) BHT, also dissolved in hexane, was added. Volumes representing 20 mg of each EPA-TAG were transferred under dim light conditions into 10 mL amber SPME vials. The prepared samples were kept under nitrogen at −80 °C. At the start of the oxidation trial (Figure 2), the samples were evaporated to dryness using nitrogen flow, and the headspace was filled with filtered air at a high flow rate for 1 min to provide oxygen for the autoxidation reaction. TAGs were oxidized at 50 °C using a Hewlett Packard 6890 Series Plus G1530A GC oven (Wilmington, DE, USA) to ensure constant temperature over the total oxidation period of 54.6 h (time points at 0.6, 12.6, 18.6, 24.6, 32.6, 40.6, 48.6, and 54.6 h). VSOPs were analyzed with HS-SPME–GC–MS at the different oxidation time points (incubation and extraction time was included in total oxidation time). Oxidation time points were chosen based on pre-tests analyzing volatiles from mixed isomers of EPA-TAGs. Immediately after the HS-SPME extraction, the samples were cooled down to room temperature, and 1 mL chloroform from Sigma-Aldrich (St. Louis, MO, USA) was added. Oxidized samples were divided for further analysis and stored under nitrogen at −80 °C. For each TAG model, also a real zero sample was prepared, which was not subjected to any heat or light. The real zero samples were handled otherwise in similar way as the oxidized samples. Three replicates of each sample type ($n = 3$) were prepared for each time point.

2.3 | Fatty Acid Analysis for Fatty Ratio Determination

Fatty acid analysis was performed by GC (Shimadzu GC-2030 from Shimadzu, Kyoto, Japan) with flame ionization detector as described in Damerau et al. [13] for DHA-TAGs. Methylation of fatty acids was based on the methanolic hydrogen chloride method of Christie and Han [21], using acetyl chloride and methanol (Sigma-Aldrich, Steinheim, Germany). For separation, a DB-23 column (60 m × 0.25 mm × 0.25 μm; Agilent Technologies, J.W. Scientific, Santa Clara, CA, USA) was used. GC conditions are reported by Damerau et al. [13]. For peak identification, external standards 37 Component FAME mix (Supelco, St. Louis, MO, USA) and GLC-490 (Nu-Check-Prep, Elysian, MN, USA) were employed. Quantification was based on internal standard concentration (triheptadecanoin from Larodan, Solna, Sweden).

2.4 | Non-Targeted Oxidomics Approach

2.4.1 | Non-Volatile Oxidation Products (HPLC–Quadrupole/Time-of-Flight [QTOF])

Non-volatile oxidation products were studied in an untargeted manner by HPLC with a quadrupole/time-of-flight (QTOF) tandem mass spectrometer (MS/MS) according to the method by Ahonen et al. [20]. EPA-TAG in chloroform of 1 mg was further diluted 1:40 (v/v) in chloroform. Elute UHPLC and Bruker

Impact II QTOF instruments from Bruker Daltonic (Bremen, Germany), equipped with a Macherey-Nagel (Düren, Germany) column Nucleodur C18 Isis (250 mm × 4.6 mm, 5 µm particle size), were used. Solvent A contained acetonitrile, water (both from Fisher Scientific, Loughborough, UK), and formic acid (VWR, Leuven, Belgium) (50:50:0.1, v/v/v) and solvent B 2-propanol (Honeywell/Riedel de Haën, Seelze, Germany), water, and formic acid (100:0.1:0.1, v/v/v). Ammonium acetate of 10 mM was added to both solvents. LC conditions and gradient program are reported by Ahonen et al. [20]. Auto MS/MS scanning mode from 60 to 2000 m/z was used, and sodium formate was applied for internal calibration. Peak picking was done by open source software MS-DIAL [22] and further processing with Bruker Compass Data Analysis 5.1 (Bruker Daltonic, Bremen, Germany). The online LIPID MAPS database (http://www.lipidmaps.org/) was used as an aid in the identification step.

2.4.2 | VSOPs (HS-SPME–GC–MS)

VSOPs were investigated by HS-SPME–GC–MS [23] using Thermo Scientific GC–MS instrument (Trace 1300 GC, ISQ 7000 single quadrupole MS, TriPlus RSH autosampler; Waltham, MA, USA) equipped with a SPB-624 capillary column (60 m × 0.25 mm × 1.4 µm, Supelco, Bellefonte, PA, USA). EPA-TAG of 20 mg (see Section 2.2) was incubated for 1 min, extracted for 30 min at 50 °C using a DVB/CAR/PDMS 50/30 µm (Supelco, Bellefonte, PA, USA) fiber, and then the fiber was desorbed for 10 min at 240 °C in the GC injection port. The GC–MS operation conditions were reported by Damerau et al. [23]. For compound identification, the NIST MS Search library (version 2.4, National Institute of Standards and Technology, Gaithersburg, MD, USA) was employed. Data were analyzed using Chromeleon 7.2.9 Chromatography Data System (Thermo Fisher Scientific, Waltham, MA, USA) and are reported as peak areas in counts per s. As a detection issue was noted for multiple samples at 18.6 h time point, the whole time point was excluded from the VSOPs data.

2.4.3 | NMR Spectroscopy

^{1}H NMR was used to analyze overall oxidative changes in an untargeted manner. Region-specific excitation was used for hydroperoxide (δ 11.5–10.5 ppm) and aldehyde (δ 10.0–9.0 ppm) regions. NMR analysis was done for the time points 24.6 and 32.6 h. The selection was based on VSOPs formation. An amount of 10 mg of oxidized EPA-TAG in chloroform was taken for analysis, and the solvent evaporated under nitrogen flow. A volume of 200 µL of dry $CDCl_3$ (Merck, Darmstadt, Germany)/DMSO-d_6 (VWR, Leuven, Belgium) (5:1; v/v) was added [24], and the sample was transferred into 3-mm NMR tube and kept at –20 °C in a desiccator until analysis. Data were collected according to the method used by Ahonen et al. [20]. For ^{1}H NMR analysis, a 600 MHz Bruker AVANCE-III NMR spectrometer (Bruker BioSpin, Switzerland) equipped with a Prodigy TCI CryoProbe and a SampleJet robotic sample changer operated at 600.16 MHz (^{1}H) at 298 K was used. Parameters of spectra recording are reported by Ahonen et al. [20]. For processing of NMR data, TopSpin 4.0.6 (Bruker Biospin, Billerica, MA, USA) and Chenomx NMR Suite 8.6 (Chenomx, Edmonton, AB, Canada) were used.

2.5 | Statistical Analysis

One-way ANOVA with Tukey's HSD test in SPSS (IBM SPSS Statistics, version 27.0.1.0, IBM, New York, USA) was used to evaluate differences of fatty acid ratios and peak area data of non-volatile and volatile oxidation products of EPA-TAGs at each time point. Differences were considered statistically significant if p value was <0.05. For an overview on the overall oxidation behavior, a PCA was formed using data from non-volatile and volatile oxidation products and manually integrated NMR data by Unscrambler X version 11.0 (Camo Analytics AS., Oslo, Norway). Data were mean-centered and weighed (1/sdev).

3 | Results and Discussion

3.1 | Identified Oxidation Products

Altogether, 17 non-volatile oxidation products were tentatively identified in EPA-containing TAGs based on their sodium $[M + Na]^+$ and ammonium $[M + NH_4]^+$ adduct fragmentation patterns (Table 1). Especially for the low-intensity compounds, identification was based on sodium adduct fragments due to their higher prevalence. Nevertheless, the ammonium adduct areas were integrated for monitoring changes in the level during the trial. The fragmentation patterns followed the principles reported earlier for DHA-containing TAGs [13]. Additions of 2–6 oxygens include mono- and polyhydroperoxides as well as cyclic structures and additions of several individual oxygen atoms to the original TAG. The addition of 16 Da (+O) can be either an epoxide or a hydroxide, whereas the addition of 14 Da (+O-2H) can correspond to an oxo group or epoxide formed next to a double bond. Similar structures with oxygen additions were detected for regio- and enantiopure EPA samples also in our previous study after in vitro digestion [25]. The most abundant fragments were the neutral loss of 20:5 acyl chain (16:0 diacylglycerol ion, m/z 551.503) and 16:0 acyl chain ion as such (m/z 313.274). Additions of oxygen to 20:5 could be detected in the masses of 16:0/20:5 diacylglycerol ions, often accompanied by losses of water. Sodiated 16:0/16:0/20:5 acyl chain cleavage products typically formed 16:0/cleaved chain diacylglycerol ions $[M + Na—RCOOH]^+$ often also with loss of water, for example, m/z 597.380 and m/z 579.379 for 16:0/16:0/15:4;O (14 Da);2O. Similar fragmentation pattern for sodiated TAGs has also been reported elsewhere [26]. Moreover, free acid of the cleaved chain with Na could be detected, for example, m/z 299.163 for 17:4;O (14 Da) $[RCOOH + Na]^+$ and 223.090 for 10:2;O2 $[RCOONa]^+$.

VSOPs are the main group of secondary oxidation products and are break down products of primary oxidation products like hydroperoxides or epoxides [14, 27]. VSOPs identified in EPA-containing TAGs are presented in Table 2. Identified VSOPs included aldehydes (15), ketones (7), acids (7), furans (4), alcohols (3), and alkenes (2). Similar to our previous study [13] on DHA-containing TAGs, aldehydes were the most abundant group of VSOPs, followed by acids and ketones. Majority of

TABLE 1 | Tentatively identified compounds from the high-performance liquid chromatography (HPLC)–quadrupole/time-of-flight (QTOF) analysis.

TAGs with oxygen additions	Mass *m/z*	Adduct *m/z*	Adduct	RT min	Main fragments *m/z*
16:0/16:0/20:5;6O	948.690	966.724	$[M + NH_4]^+$	17.75	551.506_313.275
16:0/16:0/20:5;4O	916.700	934.734	$[M + NH_4]^+$	18.52	551.504_313.270_643.447_625.438_661.459
16:0/16:0/20:5;3O	900.703	918.737	$[M + NH_4]^+$	18.88	551.505_643.459_627.446
16:0/16:0/20:5;2O	884.710	902.744	$[M + NH_4]^+$	20.75	551.505_313.275_611.473_627.464
16:0/16:0/20:5;O (14 Da)	866.701	889.691	$[M + Na]^+$	21.38	551.506_339.186_313.269_283.206
16:0/16:0/20:5;O	868.713	886.747	$[M + NH_4]^+$	22.49	551.503_613.482_283.205_301.216_313.272
16:0/16:0/20:5	852.721	870.755	$[M + NH_4]^+$	24.28	551.502_597.489_285.222_313.278_853.745
TAGs with cleaved acyl chain					
16:0/16:0/12:3;O (14 Da);2O	790.597	813.587	$[M + Na]^+$	17.55	551.504_263.083_313.279
16:0/16:0/6:1;2O	696.556	719.546	$[M + Na]^+$	17.93	551.505
16:0/16:0/15:4;O (14 Da);2O	830.628	853.618	$[M + Na]^+$	18.02	551.504_597.380_579.379_313.275
16:0/16:0/10:2;2O	750.602	773.591	$[M + Na]^+$	18.30	551.505_223.090
16:0/16:0/4:0;2O	670.541	693.530	$[M + Na]^+$	18.42	313.263_551.316
16:0/16:0/11:1;3O	782.629	805.618	$[M + Na]^+$	18.43	551.506_313.273
16:0/16:0/14:2;3O	822.660	845.649	$[M + Na]^+$	18.86	551.504_589.407_313.236
16:0/16:0/7:1;O	694.576	717.565	$[M + Na]^+$	19.02	551.502_313.282_461.324
16:0/16:0/17:4;2O	844.679	867.668	$[M + Na]^+$	19.55	317.174_611.421_551.507
16:0/16:0/17:4;O (14 Da)	826.670	849.659	$[M + Na]^+$	20.61	316.188_551.504_299.163_593.418

Note: Compound name, mass (*m/z*), adduct mass (*m/z*), retention time, and main fragments for identification in order of lowering intensity for the designated adduct.

Abbreviation: TAGs, triacylglycerols.

the identified VSOPs in EPA and DHA-containing TAGs were similar, which can be attributed to similarities in structure of EPA and DHA as both are *n*-3 PUFAs. *E*-2-butenoic acid, *E*-2-pentenoic acid, *E,Z*-3,6-nonadienal, dihydro-2(3*H*)-furanone, and 2-propylcyclohexanone were only detected in EPA-containing TAGs, whereas 2-methyl-2-pentanol, 1-nonen-3-ol, and nonanal were only identified in DHA-containing TAGs. This difference could be based on pathway differences between oxidation of EPA and DHA. However, also differences in oxidation level and chromatographic separation between the studies could play a role. 3,6-Nonadienal and dihydro-2(3*H*)-furanone were also identified for oxidized DHA in our previous study analyzing VSOPs from only DHA-containing TAGs [28]. Although all identified VSOPs were present in all samples regardless of enantiomer, their amount formed was different for the different enantiomers (see Sections 3.2 and 3.3).

^{1}H NMR was used to observe overall changes in structure and functional groups occurring during oxidation. Data were only collected from two selective time points, 24.6 and 32.6 h, during the propagation phase. ^{1}H NMR spectra are shown in Figures S1–S3. Time points were chosen based on observed formation of VSOPs. Signal identifications were made based on previous studies on DHA [13, 20], linoleic acid [7], and edible oils [22, 29] and are reported in Table 3. Similar to our previous study [13] on DHA-containing TAGs, ^{1}H NMR spectra can be used to clearly distinguish between PUFAs in the middle (*sn*-2) and outer positions (*sn*-1/3), confirming high purity of the synthesized TAGs. Both (*Z,E*) and (*E,E*)-conjugated double bonds associated with hydroperoxyl group were also detected for EPA, whereas in our previous study [13] on DHA-containing TAGs, only (*Z,E*)-conjugated bonds were detected. Similar observations of signals related to both (*E,Z*)- and (*E,E*)-conjugated double bonds associated with hydroperoxyl group were made by Wang et al. [7] for linoleic acid oxidation. The identification of signals of (*E,E*)-conjugated double bonds associated with hydroperoxyl group, 4,5-epoxy-(*E*)-2-alkenals, 4-hydroxy-(*E*)-2-alkenals, and (*E,E*)-2,4-alkadienals in this study suggested higher oxidation levels were analyzed in this study than in our previous one on DHA-containing TAGs [13], as (*E,E*)-conjugated double bonds are formed under H donor-lacking conditions, which are favored in the later stages of oxidation [30].

3.2 | Overall Oxidation Behavior

One general oxidation indicator is the fatty acid consumption during oxidation. In the current study, EPA consumption was reported as changes in the ratio of EPA to C16:0 in TAG samples as the content of C16:0 was expected to remain stable during

TABLE 2 | Volatile compounds identified by solid-phase micro extraction with gas chromatography–mass spectrometry (SPME—GC—MS) in all oxidized eicosapentaenoic acid (EPA) triacylglycerols with butylated hydroxytoluene (BHT).

Compound group	Compound	*m/z*[a]	Match[b]	RT (min)
Acids (7)	Formic acid	44, 45, 46	920	15.7
	Acetic acid	43, 45, 60	959	17.3
	Propanoic acid	45, 57, 73, 74	975	21.8
	Butanoic acid	41, 60, 73	954	25.4
	2-Butenoic acid (*E*)	41, 57, 68, 86	903	27.2
	2-Petenoic acid (*E*)	55, 76, 82, 100	926	30.9
	3-Hexenoic acid	41, 55, 68, 114	906	33.5
Alcohols (3)	1-Penten-3-ol	41, 57	891	19.4
	2-Penten-1-ol (*Z*)	41, 44, 57, 68, 86	864	23.5
	2-Penten-1-ol (*E*)	41, 44, 57, 68, 86	912	23.8
Aldehydes (15)	Acetaldehyde	42, 43, 44	932	6.5
	2-Propenal	53, 55, 56	942	9.7
	Propanal	57, 58, 59	901	9.9
	Butanal	43, 57, 72	948	14.5
	2-Butenal (*Z*)	41, 69, 70	918	18.1
	2-Pentenal (*Z*)	41, 55, 83, 84	899	22.3
	2-Pentenal (*E*)	41, 55, 83, 84	910	23.0
	3-Hexenal	41, 69, 55	841	24.4
	2-Hexenal (*E*)	41, 55, 69, 83, 98	850	27.3
	2,4-Hexadienal (*E,E*)	53, 67, 81, 96	887	29.9
	4-Oxohex-2-enal	55, 69, 83, 112	933	32.4
	2,4-Heptadienal (*E,Z*)	41, 53, 81, 110	922	33.1
	2,4-Heptadienal (*E,E*)	41, 53, 81, 110	911	33.7
	3,6-Nonadienal (*E,Z*)	41, 55, 67, 79, 95, 123	867	36.1
	Cis-4,5-epoxy-(*E*)-2-decenal[c]	55, 68, 81, 139, 152	768	36.6
	Trans-4,5-epoxy-(*E*)-2-decenal[c]	55, 68, 81, 139, 152	809	36.8
Ketones (7)	1-Penten-3-one	55, 57, 84	884	19.2
	1-Hydroxy-2-butanone	57, 88	890	24.3
	Dihydro-2 (3*H*)-furanone	42, 56, 86	946	32.0
	5-Methyl-2 (5*H*)-furanone	43, 55, 69, 83, 98	935	32.9
	3, 5-Octadien-2-one (*E, Z*)	43, 81, 95, 124	920	35.5
	3, 5-Octadien-2-one (*E, E*)	43, 81, 95, 124	926	36.5
	5-Ethyl-2 (5*H*)-furanone	55, 67, 83, 112	884	36.3
	2-Propylcyclohexanone[c]	42, 54, 55, 70, 83, 98	801	41.6
Furans (4)	2-Methylfuran	50, 53, 82	868	14.0
	2-Ethylfuran	53, 81, 96	942	18.8
	2-Hydroxymethyl-tetrahydrofuran	43, 57, 71, 99	856	24.9
	Trans-2-(2-pentenyl)furan	79, 81, 94, 107, 136	903	31.6

(Continues)

TABLE 2 | (Continued)

Compound group	Compound	*m/z*[a]	Match[b]	RT (min)
Dienes/tirenes (2)	2,4-Nonadiene (*E,E*)[c]	41, 68, 81, 95, 124	785	29.4
	4,6,9-Nonadecatriene (*Z,Z,Z*)[c]	41, 55, 67, 79, 91, 105, 121, 219	784	46.4

Abbreviation: RT, retention time.

[a]Main fragments for identification.

[b]NIST match number.

[c]Tentatively identified (NIST match < 850).

the selected oxidation conditions. Non-oxidized samples had an EPA to C16:0 weight ratio of approximately 0.59 (Figure 3). The ratio of EPA to C16:0 in both 1ET and 3ET started to slightly decrease at 12.6 h, showing the start of EPA consumption. The ratio in 3ET decreased significantly slower at 18.6 and 24.6 h than in 1ET, and both significantly faster than in 2ET (Figure 3), which indicated a higher oxidation rate for 1ET compared to 3ET. Even at 48.6 h, a significantly higher ratio for 3ET was measured than for 1ET. A similar trend was also observed for DHA without antioxidant addition [13]. In 2ET, the ratio of EPA to C16:0 was stable during the oxidation trial, showing almost no consumption of EPA (Figure 3). Therefore, 2ET showed a significantly higher oxidative stability compared to 1ET and 3ET.

Superior stability for EPA/DHA at *sn*-2 position in TAGs with two saturated fatty acids has been reported in several earlier studies in neat oil [9, 11, 13], emulsion [12], and aqueous buffer [10]. However, when oxidized in benzene at 37 °C, no difference was found in the stability of EPA in the *sn*-2 or *sn*-1/3 positions in TAGs along with two palmitic acids [10]. Compared to DHA-containing TAGs [13], the difference in stability between *sn*-2 and *sn*-1(3) was much more pronounced for EPA than DHA based on ratio of PUFA to C16:0. This may be related to overall higher oxidative stability of EPA compared to DHA. Some studies have shown that when TAGs consist of two unsaturated FAs and one saturated/less unsaturated FA, the unsaturated FAs are more protected when located at *sn*-1 and *sn*-3 positions compared to those adjacently placed at *sn*-2 and *sn*-1/3 positions [4, 5, 10] due to the oxidative interactions between the neighboring acyl chains. In the case of only one EPA at *sn*-1/2/3 position and two saturated FAs in the remaining positions of a single TAG, the interactions within the same TAG are similar. However, the protective effect of *sn*-2 position might be related to interactions with neighboring TAGs so that the FA in the *sn*-2 position interacts less with the *sn*-2 position of other TAGs compared to *sn*-1/3 positions, as was suggested already in 1967 by Raghuveer and Hammond [31].

Although the consumption of EPA is a clear indicator of oxidation, it is not a sensitive one. Therefore, for further analysis of overall oxidation behavior, a PCA model of selected non-volatile and volatile oxidation products was comprised (Figure 4) using the oxidomics approach. For non-volatile oxidation products, area data of M+O, M+2O, M+4O, M+14, 16:0/16:0/17:4;O2, 16:0/16:0/7:1;O, 16:0/16:0/10:2;O2, 16:0/16:0/4:0;O2 and 16:0/16:0/12:3;O(oxo)O2 was used. For the VSOPs area data of acetaldehyde, 2-propenal, propanal, 2-pentenal (*Z* and *E* combined), 4-oxohex-2-enal, 2,4-heptadienal (*E,Z* and *E,E* combined), 1-penten-3-one, 1-hydroxy-2-butanone, dihydro-2(3*H*)-furanone, 5-ethyl-2(5*H*)-furanone, 2-propylcyclohexanone, 1-penten-3-ol, formic acid, acetic acid, propanoic acid, 2-ethylfuran, and *trans*-2-(2-pentenyl)furan was included. Selected compounds were chosen based on abundance and suitability as oxidation indicators based on representation of possible oxidation pathways.

PC-1 accounted for 78%, whereas PC-2 accounted for 15% of the variation (Figure 4). The loadings of oxidation products were all on the positive side of PC-1, which means the further right a sample is located on PC-1, the more oxidized it is. Differences in the loadings of PC-2 indicated variations in the formation time of oxidation products. The more positive the loading of PC-2, the later the oxidation product was formed. Additions of oxygen and earlier formed volatiles, like 2-ethylfuran, had negative loadings on PC-2, whereas later formed volatiles like acids had positive loadings on PC-2 (Figure 4, Loadings). In general, all replicates grouped together (Figure 4, Scores). All time points of 2ET and 0.6 and 12.6 h of 1ET and 3ET grouped together on negative side of PC-1, indicating low formation of oxidation products. This finding was in-line with the degradation of EPA (Figure 3). All time points from 24.6 h onwards of 1ET and 3ET were found on the positive side of PC-1, shifting from the negative side of PC-2 to the positive side as time progressed (Figure 4, Scores). 1ET and 3ET grouped together according to time point. However, 3ET was always found further left on PC-1 and lower on PC-2 than 1ET, indicating higher oxidative stability of *sn*-3 compared of *sn*-1 for EPA. This was most notable for 24.6 and 48.6 h, which was in-line with behavior of the ratio of EPA to C16:0 at these time points (Figure 3).

Overall, the PCA of selected oxidation products confirmed the high oxidative stability of EPA in *sn*-2, attributed to lower formation of oxidation products likely due to steric hindrance. The PCA also indicated a minor difference in oxidation behavior between EPA in *sn*-1 and *sn*-3. Our group observed similar oxidation behavior during in vitro digestion of the same regio- and enantiopure EPA-containing TAGs by analyzing non-volatile oxidation compounds by HPLC–QTOF [25]. EPA in *sn*-2 was most oxidatively stable, followed by *sn*-3 and *sn*-1 under the prooxidative conditions of the gastrointestinal tract.

3.3 | Evaluation of Oxidative Stability Differences Based on Selected Compounds and Time Points

For a detailed assessment of the differences in oxidation behavior, a more detailed data analysis of selected oxidation products at selected time points was conducted. The oxidation products were

TABLE 3 | Assignments of integrated signals of nuclear magnetic resonance (^{1}H NMR) spectra of eicosapentaenoic acid (EPA)-triacylglycerols (TAGs). Spectra were recorded in $CDCl_3$/DMSO-d_6 (5:1) at 298 K (600 MHz).

Chemical shift (ppm)	Variable ID in Figure 7	Multiplicity	Type of proton	Compound group
0.88	0.88	t	–C**H**$_3$	Methyl group in C16:0
0.97	0.97	t	–C**H**$_3$	Methyl group in EPA
1.23–1.32	1.28	m	–(C**H**$_2$)$_n$–	Methylene group
1.60	1.60	quint	–OCO–CH$_2$–C**H**$_2$–	Methylene group beta to acyl group in C16:0 (EPA *sn*-2)
1.56–1.63	1.60	m	–OCO–CH$_2$–C**H**$_2$–	Methylene group beta to acyl group in C16:0 (EPA *sn*-1 [3])
1.69	1.69	quint	–OCO–CH$_2$–C**H**2–	Methylene group beta to acyl group in EPA
1.94–2.01	1.98	m	CHO–CH=CH–CHOOH–(C**H**$_2$)$_n$	Methylene group in 4-hydroperoxy-(*E*)-2-alkenals
2.03–2.14	2.09	m	–C**H**$_2$–CH=CH–	Allylic methylene group
2.30	2.31	t	–OCO–C**H**$_2$–CH$_2$–	Methylene group alpha to acyl group (EPA *sn*-2)
2.28–2.33	2.31	td	–OCO–C**H**$_2$–CH$_2$–	Methylene group alpha to acyl group (EPA *sn*-1 [3])
2.37–2.43	2.40	m	–OCO–C**H**$_2$–C**H**$_2$–	EPA acyl chain
2.60	2.60	m		Unassigned[a]
2.77–2.88	2.83	m	=CH–C**H**$_2$–CH=	Diallylic methylene group
4.11–4.16	4.14	dd	–C**H**$_2$OCOR	Glyceryl group (EPA *sn*-2)
4.10–4.17	4.14	ddd	–C**H**$_2$OCOR	Glyceryl group (EPA *sn*-1 [3])
4.25–4.32	4.30	dd	–C**H**$_2$OCOR	Glyceryl group (EPA *sn*-2)
4.26–4.33	4.30	ddd	–C**H**$_2$OCOR	Glyceryl group (EPA *sn*-1 [3])
5.21–5.26	5.24	tt	>C**H**OCOR	Glyceryl group
5.27–5.32	5.30	m	–C**H**=C**H**–	Olefinic group
5.32–5.42	5.37	m	–C**H**=C**H**–	Olefinic group
5.44–5.55	5.50	m	–CHOOH–CH=CH–CH=C**H**– (*E*/*Z*) and (*E*/*E*)	Conjugated double bonds associated with hydroperoxyl group
5.59–5.68	5.64	m	–CHOOH–C**H**=CH–CH=CH– (*E*/*Z*)	
5.68–5.73	5.71	m	–CHOOH–C**H**=CH–CH=CH– (*E*/*E*)	
5.83–5.96	5.90	m	–CHOOH–CH=CH–C**H**=CH– (*E*/*Z*)	
5.96–6.06	6.01	m	CHOOH–CH=CH–C**H**=CH– (*E*/*E*)	
6.14–6.24	6.19	m	–CHOOH–CH=C**H**–CH=CH– (*E*/*E*)	
6.24–6.33	6.29	m	CHOOH–CH=C**H**–CH=CH– (*E*/*Z*)	
6.48–6.58	6.53	dd	CHO–C**H**=CH–	4, 5-Epoxy-(*E*)-2-alkenals

(Continues)

TABLE 3 | (Continued)

Chemical shift (ppm)	Variable ID in Figure 7	Multiplicity	Type of proton	Compound group
6.58–6.66	6.62	dd	CHO–CH=C**H**–	4, 5-Epoxy-(*E*)-2-alkenals
6.84–6.89	6.87	dd	CHO–CH=C**H**–	4-Hydroxy-(*E*)-2-alkenals
7.08–7.16	7.12	m	CHO–CH=C**H**–	(*E,E*)-2,4-alkadienals
9.00–10.00	9.5	m	–C**H**O	Aldehyde groups
10.50–11.50	11	m	–CHOO**H**	Hydroperoxyl groups

Abbreviations: dd, doublet of doublets; ddd, doublet of doublet of doublets; m, multiplet; quint, quintet; t, triplet; td, triplet of doublets; tt, triplet of triplets.
[a]Possibly an (*E*)-9,10-epoxy group according to Hwang, H.-S. Application of NMR Spectroscopy for Foods and Lipids. In Advances in NMR Spectroscopy for Lipid Oxidation Assessment; Hwang, H.-S., Ed.; SpringerBriefs in Food, Health, and Nutrition; Springer International Publishing: Cham, Switzerland, 2017; pp. 33–43.

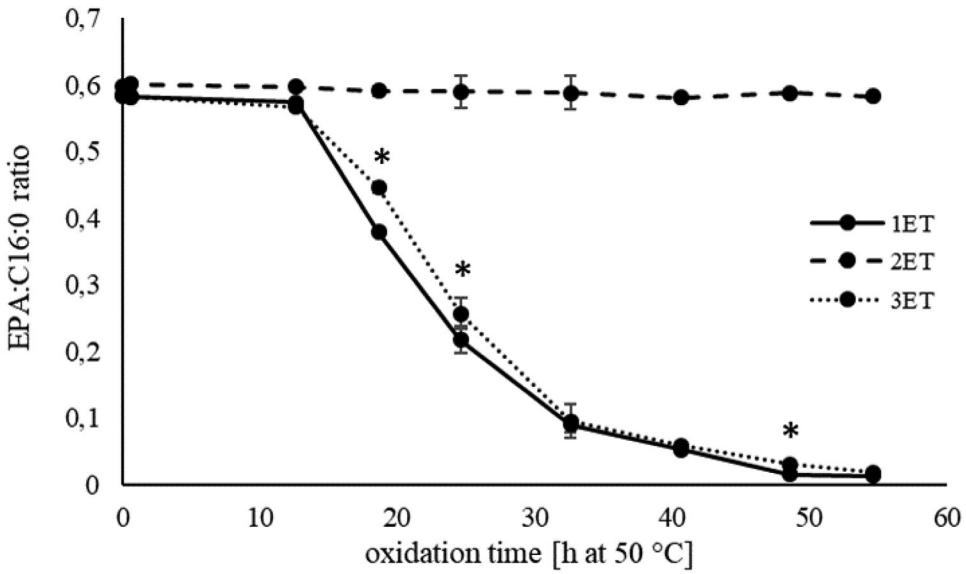

FIGURE 3 | EPA to palmitic acid (C16:0) weight ratio development during the 54.6 h oxidation trial at 50 °C for EPA containing triacylglycerols with EPA in *sn*-1 (1ET), *sn*-2 (2ET), and *sn*-3 (3ET) position ($n = 3$). Time points marked with * showed a statistically significant difference ($p < 0.05$) between *sn*-1 and *sn*-3. At all time points, except 0 h, *sn*-2 differed statistically significantly from *sn*-1/3. EPA, eicosapentaenoic acid.

selected on the basis of their impact on PCA model (Figure 4). This difference is of high interest as this is the first time this could be studied for EPA. It was expected that in an achiral environment, PUFAs in *sn*-1 and *sn*-3 behave identically.

The level evolution for non-volatile oxidation products M+O, M+2O, M+4O, and 16:0/16:0/7:1;O are presented in Figure 5. 2ET did not produce any significant amounts of non-volatile oxidation products during the 54.6 h oxidation period, although for M+O, M+14 Da, M+2O, and 16:0/16:0/7:1;O some formation was observed, which is in-line with the discussion in Section 3.2. From 12.6 to 18.6 h, the epoxide/hydroxide (M+O) level increased significantly faster in the 1ET samples compared to 3ET (Figure 5), thus indicating better stability for the *sn*-3 enantiomer. A similar trend was observed for M+2O and M+14 Da (oxo/epoxy, data not shown). Moreover, the M+4O levels showed improved stability in the 3ET samples compared to 1ET, with the highest level a bit later than in the above-mentioned oxidation products, at 32.6 h. In the acyl chain cleavage product levels, the difference between 3ET and 1ET was less pronounced but still statistically significant for 16:0/16:0/7:1;O at 18.6 h (Figure 5). The compounds 16:0/16:0/10:2;O2, 16:0/16:0/4:0;O2, and 16:0/16:0/12:3;O(oxo)O2 behaved similarly to 16:0/16:0/7:1;O, whereas 16:0/16:0/17:4;O2 showed a trend similar to M+4O, with the highest formation rates at 32.6 h and steep decrease after that. By peak area, this was also the most abundant acyl chain cleavage product. In our previous study with similar regio- and enantiopure samples containing DHA and palmitic acid, the most abundant non-volatile acyl chain cleavage product was 16:0/16:0/19:5;O2 [13]. 16:0/16:0/17:4;O2 from EPA and 16:0/16:0/19:5;O2 from DHA could form through propanal cleavage from 18/20-LO$^{\bullet}$ of former dihydroperoxide.

For some of the VSOPs, an induction period could be determined, but for most, more time points in earlier stages of oxidation would have been needed in the case of 1ET and 3ET (Figure 6). In the case of 2ET, a 12.6 h induction period could be determined for most volatiles, except for 2-ethylfuran and 2-propylcyclohexanone where formation was earlier and later than 12.6 h, respectively. Overall, the formation of VSOPs was significantly lower in 2ET

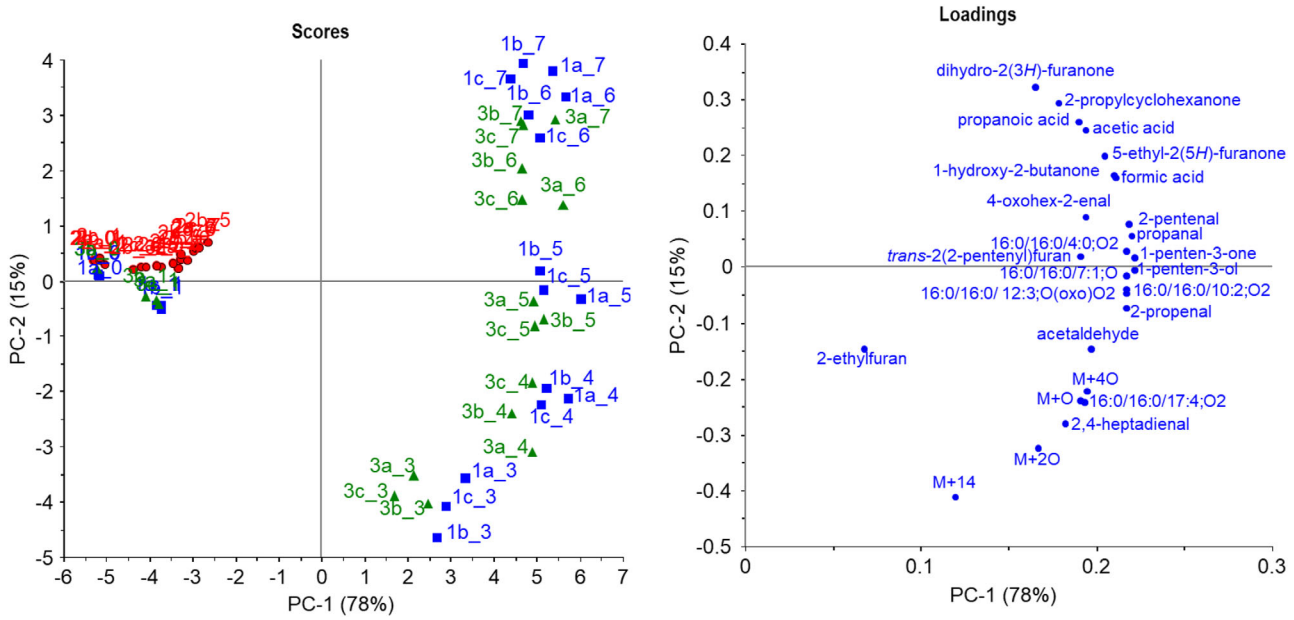

FIGURE 4 | PCA model for integrated non-volatile and volatile oxidation product area data for eicosapentaenoic acid (EPA)-containing triacylglycerols with EPA in *sn*-1 (1, blue), *sn*-2 (2, red), and *sn*-3 (3, green) position at different time points (0.6 h = 0, 12.6 h = 1, 24.6 h = 3, 32.6 h = 4, 40.6 h = 5, 48.6 h = 6, and 54.6 h = 7) ($n = 3$, marked as a, b, c).

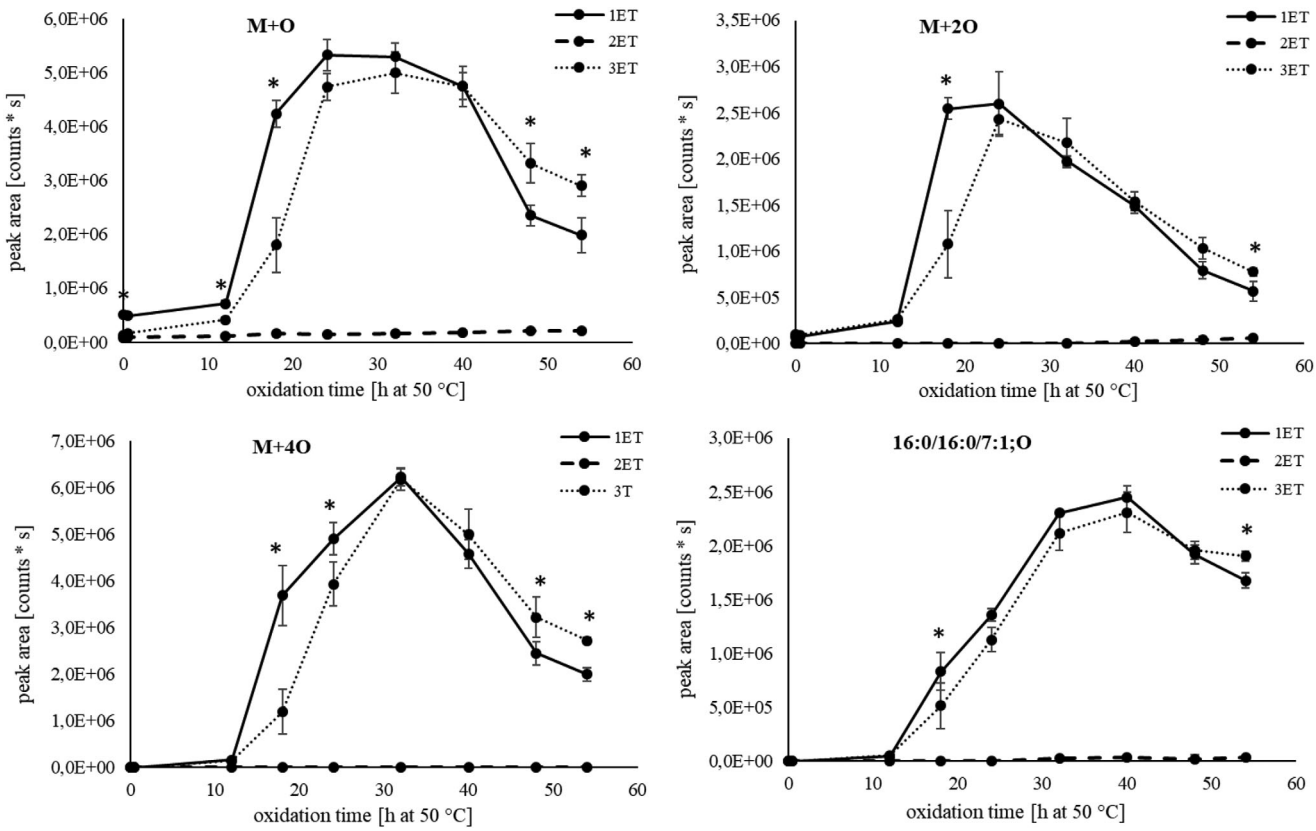

FIGURE 5 | Peak areas of oxidation products M+O, M+2O, M+4O, and 2×16:0+7:1;O, in the eicosapentaenoic acid (EPA)-containing triacylglycerols oxidized in the 54.6 h oxidation trial at 50 °C in the dark (1ET:*sn*-1 EPA, 2ET:*sn*-2 EPA, and 3ET:*sn*-3 EPA). Values are mean ± standard deviation of three replicates. Time points marked with * showed a statistically significant difference ($p < 0.05$) between *sn*-1 and *sn*-3.

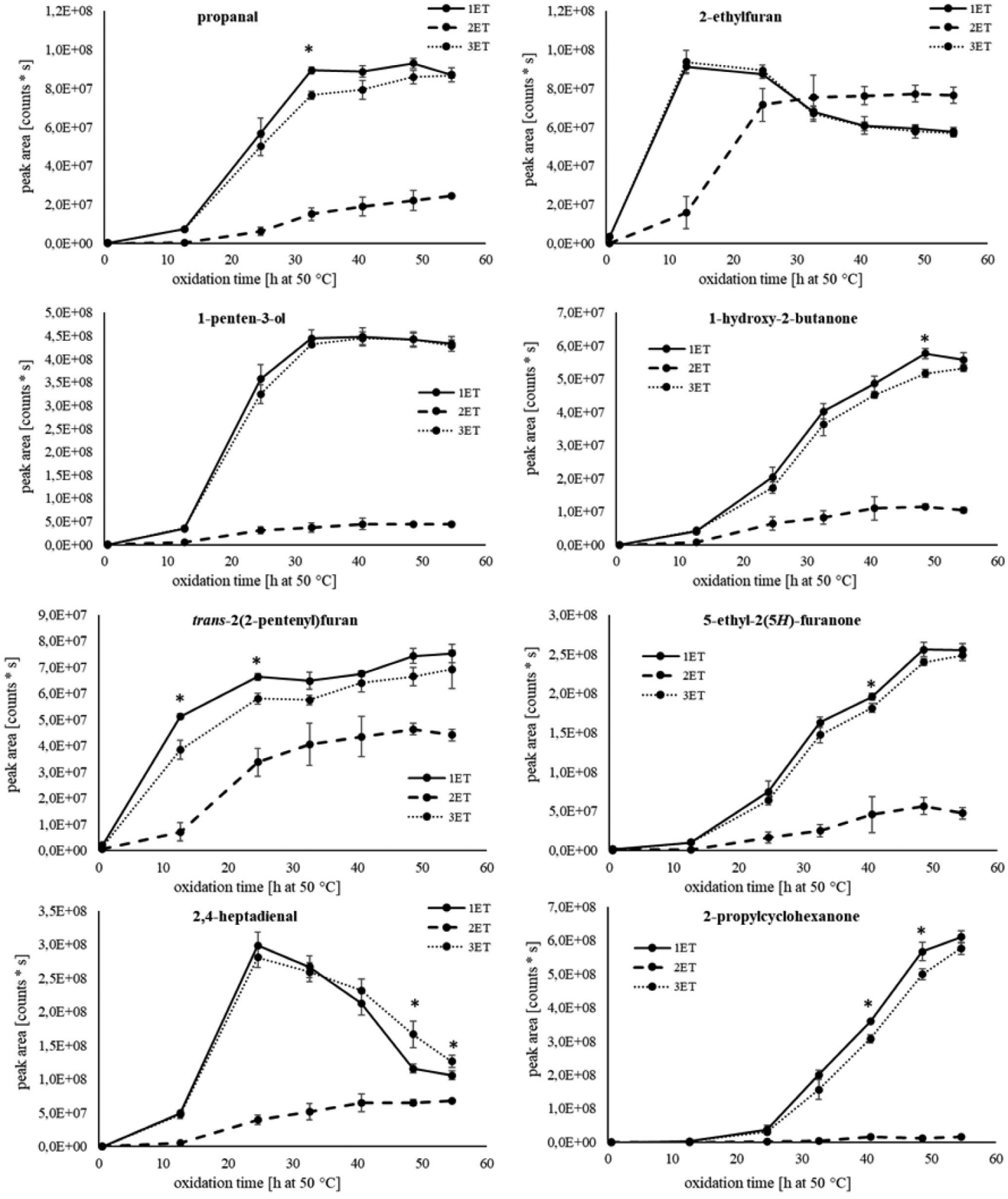

FIGURE 6 | Peak areas of propanal, 2-ethylfuran, 1-penten-3-ol, 1-hydroxy-2-butanone, *trans*-2(2-pentenyl)furan, 5-ethyl-2 (5*H*)-furanone, 2,4-heptadienal (*E,Z* and *E,E* combined), and 2-propylcyclohexanone in the 54.6 h oxidation trial at 50 °C for eicosapentaenoic acid (EPA)-containing triacylglycerols with EPA in *sn*-1 (1ET), *sn*-2 (2ET), and *sn*-3 (3ET) position ($n = 3$). Time points marked with * showed a statistically significant difference ($p < 0.05$) between *sn*-1 and *sn*-3. At all time points, except at 0.6 h for all compounds and at 32.6 h for 2-ethylfuran, *sn*-2 differed statistically significantly from *sn*-1/3.

than in 1ET and 3ET as expected based on the non-volatile oxidation product results. Only in later time points for 2-ethylfuran was a greater content detected in 2ET than in 1ET and 3ET (Figure 6), which was related to similar but delayed behavior as seen for 1ET and 3ET. Although the formation of VSOPs was low in 2ET, it was still higher than expected based on non-volatile and ^{1}H NMR results. No hydroperoxide signals were measured for 2ET with ^{1}H NMR, although regio-specific excitation was used. This discrepancy could be attributed to differences in sensitivity of methods to detect oxidation products. HS-SPME–GC–MS was found the most sensitive method, followed by HPLC–QTOF. ^{1}H NMR was least sensitive method used for the detection of oxidation products. Part of the sensitivity issue is also related to the nature of oxidation products measured with these methods.

Propanal and 1-penten-3-ol showed a similar behavior for 1ET and 3ET (Figure 6). In both cases, the formation increased greatly between 12.6 and 24.6 h, and after 32.6 h, the content leveled out. The content in 3ET was slightly lower than in 1ET at 12.6 and 32.6 h. For 2ET, a significantly lower formation than for 1ET/3ET was seen for all time points. A similar behavior as for propanal and 1-penten-3-ol was also seen for 2-propenal, 1-penten-3-one, and 2-pentenal, which are formed by similar pathways. 2-Ethylfuran increased significantly from the start of the oxidation trial in 1ET and 3ET and started to decrease already after 24.6 h (Figure 6), which indicated further reactions. No significant difference was detected between 1ET and 3ET for 2-ethylfuran. For 2ET, a higher formation of 2-ethylfuran was detected than for 1ET/3ET after 32.6 h. 2-ethylfuran behaved uniquely compared to other VSOPs. For 1-hydroxy-2-butanone and 5-ethyl-2(5*H*)-furanone, a steady rise was observed for 1ET and 3ET between 12.6 and 48.6 h. Throughout the oxidation period, the content in 3ET was a bit lower than in 1ET. However, it was not significant for most time points, whereas the content for 2ET was throughout the oxidation trial significantly lower than for the other enantiomers. A similar behavior was also displayed by formic acid. *Trans*-2-(2-pentenyl)furan, which showed a similar formation pattern to 4-oxohex-2-enal, increased from start until the end of the oxidation trial (Figure 6). The content in 3ET was significantly lower than in 1ET at 12.6 and 24.6 h and in 2ET than in 1ET/3ET for the whole time. For both 1ET and 3ET, the amount of 2,4-heptadienal built up until 24.6 h and decreased afterward. For 3ET, the reduction was significantly slower than for 1ET. A similar oxidation pattern as for 2,4-heptadienal was also observed for acetaldehyde, which reacted further to acetic acid. 2-Propylcyclohexanone showed the slowest formation of VSOPs (Figure 6). For both 1ET and 3ET, a clear induction period of 12.6 h could be determined. Afterward, the content increased until the end of oxidation trial. For 1ET, the content was significantly higher than for 3ET at 40.6 and 48.6 h. Interestingly, almost no formation of 2-propylcyclohexanone was detected in 2ET. This and the late onset point to a different formation pathway than most other VSOPs. Dihydro-2(3*H*)-furanone showed similar pattern as 2-propylcyclohexanone. Overall, the detailed data on VSOPs supports the fact that EPA was more stable in *sn*-3 than in *sn*-1 at some time points. However, the distinction was a bit less clear than for non-volatile products. 2ET showed always significantly less formation than 1ET and 3ET at all time points expect for later time points of 2-ethylfuran. Data on same VSOPs in EPA and DHA-containing TAGs [13] showed comparable formation patterns further, supporting similarities in oxidation patterns of *n*-3 PUFAs. However, the extent of oxidation was greater in this study than in our previous one [13] on DHA. This was also seen in Figure 3, as almost no EPA was left in this oxidation trial.

A PCA combining the data of non-volatile and volatile oxidation products with ^{1}H NMR data was comprised for selected time points (24.6 and 32.6 h) of the propagation phase. For the ^{1}H NMR data, only signals that are affected by oxidation process (either formed or consumed) were considered. The PCA model showing the distribution of samples and selected oxidation products at 24.6 and 32.6 h is presented in Figure 7. PC-1, accounting for 85% of the variation between samples, separates based on earlier formed oxidation products and signals of structures consumed during oxidation on the negative side and later formed oxidation products and signals of structures formed during oxidation on the positive side. The variance of 9% in PC-2 was mainly due to higher content of detected products/signals. ^{1}H NMR signals are found near to oxidation products with corresponding structures, for example, signal of aldehyde region (9.5) close to 2-propenal and propanal (Figure 7, Loadings). All replicates of 2ET for both time points were located on negative side of PC-1 and positive side of PC-2 (Figure 7, Scores) associated with diallylic methylene group, olefinic group, methyl group in EPA, methylene group beta to acyl group in EPA, and allylic methylene group (Figure 7, Loadings), which are structures consumed by oxidation. At 24.6 h, both 1ET and 3ET grouped on positive side of PC-1 and negative side of PC-2 (Figure 7, Scores) related to early formed VSOPs, M+2O, M+14, and signals of hydroperoxyl groups. Two replicates of 3ET were located more toward the negative side of PC-1 than replicates of 1ET, indicating lower amounts of these compounds/structures for 3ET than 1ET. At 32.6 h, both 1ET and 3ET were found on the positive side of both PC-1 and -2 (Figure 7, Scores). Both were associated with later formed VSOPs like 5-ethyl-2(5*H*)-furanone, 2-propylcyclohexanone, or acids and other cleavage products like 16:0/16:0/4:0;O2 and 16:0/16:0/7:1;O (Figure 7, Loadings). Two replicates of 3ET were located lower than replicates of 1ET, more related to propanal, 2-propanal, and signals of conjugated double bonds associated with hydroperoxyl group.

The evaluation of oxidative stability based on selected compounds and time points 24.6 and 32.6 h both supported the previous findings on overall oxidative stability (**3.2**) that *sn*-2 is significantly more stable than *sn*-1 and *sn*-3. Some selective compounds, at certain time points, indicated better stability for *sn*-3 than *sn*-1. Although there was a tendency for better stability of *sn*-3 than *sn*-1 seen for some replicates in the PCAs (Figures 4 and 7), no clear distinction of *sn*-1 and *sn*-3 could be drawn considering the PCAs, which are comprised of data of multiple oxidation compounds measured by different methods, which represents a more complete picture of oxidation behavior than selected compounds. A plausible explanation for the unexpected difference in oxidation behavior observed between *sn*-1 and *sn*-3 might be due to trace-level prooxidative impurities. The synthetic pathways and procedures followed for preparing the two TAG enantiomers, *sn*-1 and *sn*-3, were identical, involving the same chemicals, reagents, and solvents. The only difference is the use of the two enantiomeric precursors, namely (*R*)-solketal for the *sn*-1 enantiomer and (*S*)-solketal for the *sn*-3 enantiomer. However, the origin of the two chiral precursors obtained from

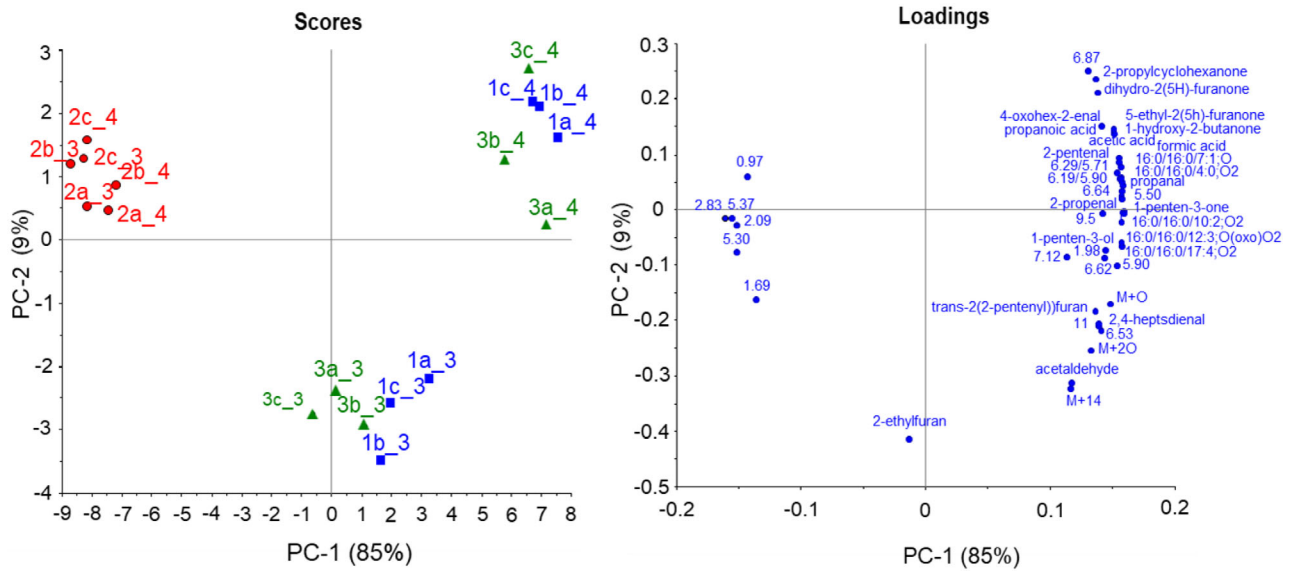

FIGURE 7 | PCA model (PC-1 vs. PC-2) for integrated non-volatile and volatile oxidation product area data and NMR data integrals of the aldehyde (10–9 ppm), hydroperoxide (11.5–10.5 ppm), and selected lipid structural regions (see Table 3) for eicosapentaenoic acid (EPA) containing triacylglycerols with EPA in *sn*-1 (1, blue), *sn*-2 (2, red), and *sn*-3 (3, green) position at two selected time points (24.6 h = 3, 32.6 h = 4) ($n = 3$ marked as a, b, c).

the chiral pool of nature is different, and that could explain the different trace levels of prooxidative impurities between the two TAG enantiomers. This is supported by similar trends obtained in our previous studies involving DHA with the *sn*-3 enantiomer showing slightly higher stability than the *sn*-1 enantiomer under achiral conditions. In that case, the same chiral solketal precursors were used as in the synthesis of 1ET and 3ET. It is also of interest that DHA was observed to be more stable when located in the *sn*-1 position as compared to the *sn*-3 position when performing the oxidative stability studies in the presence of a chiral antioxidant.

4 | Conclusion

EPA was clearly the most stable in *sn*-2 position in TAGs as neat oil. Regioisomeric differences in oxidation rate may be ascribed to intermolecular interactions between the acyl chains and possible steric hindrance for hydroperoxide formation. Oxidation products and patterns of EPA-containing TAGs were similar to those confirmed earlier for DHA-containing TAGs. Therefore, these oxidation products, for example, propanal, 1-penten-3-ol, 2,4-heptadienal, and 5-ethyl-2(5*H*)-furanone, could be used as oxidation indicator compounds for *n*-3 PUFAs as they showed similar formation behavior for both EPA and DHA. Although the stability of EPA in *sn*-1 and *sn*-3 was more similar compared to the stability of EPA in *sn*-2, statistically better stability in *sn*-3 than in *sn*-1 could be interpreted based on some oxidation compounds at certain time points. This behavior was most pronounced in the earlier propagation phase. However, no clear distinction of *sn*-1 and *sn*-3 could be drawn considering the PCAs represent a more complete picture of oxidation behavior than selected compounds. As there are no known molecular mechanisms for the differences in the oxidative stability between *sn*-1 and *sn*-3 without another chiral molecule present, the logical interpretation is that the observed difference arose from a difference in minor undetected and unidentified prooxidant contaminants, possibly originating from the raw materials. Regarding the EPA in the *sn*-2 position, the hypothesis of this study could be proven as the oxidative stability of EPA was similarly dependent on its location in the glycerol backbone as seen before for DHA. Further studies should be continued in chiral environments and in other systems like emulsions. The results of this study are significant for oxidative stability of EPA-rich marine oil concentrates produced by re-structuring of TAGs to be used as food supplements or in food fortification.

Author Contributions

Annelie Damerau: conceptualization, methodology, formal analysis, investigation, writing – original draft, writing – review and editing, visualization, supervision; funding acquisition. **Eija Ahonen**: methodology, formal analysis, investigation, writing – original draft, writing – review and editing, visualization, funding acquisition. **Maaria Kortesniemi**: methodology, investigation, writing – review and editing, supervision, visualization. **Haraldur G. Gudmundsson**: methodology, writing – review and editing. **Baoru Yang**: resources, writing – review and editing. **Gudmundur G. Haraldsson**: conceptualization, methodology, writing – review and editing, resources, supervision. **Kaisa M. Linderborg**: conceptualization, methodology, resources, writing – review and editing, supervision, project administration, funding acquisition.

Acknowledgments

The authors would like to thank Nashmil Palani for assistance with part of the practical work related to fatty acid analysis. Personal financial grant to Annelie Damerau from the Finnish Cultural Foundation is acknowledged. Further, personal financial grant to Eija Ahonen from Niemi Foundation is acknowledged. This work entity was carried out as part of the Research Council of Finland funded project "Omics of oxidation—Solutions for better quality of docosahexaenoic and eicosapentaenoic acids" (grant number 315274, PI Kaisa M. Linderborg).

Conflicts of Interest

The authors declare no conflicts of interest.

Data Availability Statement

Data of the chemical analyses are available from the corresponding authors upon reasonable request.

References

1. R. K. Saini and Y. S. Keum, "Omega-3 and Omega-6 Polyunsaturated Fatty Acids: Dietary Sources, Metabolism, and Significance—A Review," *Life Sciences* 203 (2018): 255–267, https://doi.org/10.1016/j.lfs.2018.04.049.

2. S. A. Vieira, G. Zhang, and E. A. Decker, "Biological Implications of Lipid Oxidation Products," *Journal of the American Oil Chemists' Society* 94 (2017): 339–351, https://doi.org/10.1007/s11746-017-2958-2.

3. A. Rundblad, K. B. Holven, I. Ottestad, and M. C. Myhrstad, "High-Quality Fish Oil Has a More Favourable Effect Than Oxidised Fish Oil on Intermediate-Density Lipoprotein and LDL Subclasses: A Randomized Controlled Trial," *British Journal of Nutrition* 117 (2017): 1291–1298.

4. E. N. Frankel, E. Selke, W. E. Neff, and K. Miyashita, "Autoxidation of Polyunsaturated Triacylglycerols. IV. Volatile Decomposition Products From Triacylglycerols Containing Linoleate and Linolenate," *Lipids* 27 (1992): 442–446, https://doi.org/10.1007/BF02536386.

5. K. Miyashita, E. N. Frankel, W. E. Neff, and R. A. Awl, "Autoxidation of Polyunsaturated Triacylglycerols. III. Synthetic Triacylglycerols Containing Linoleate and Linolenate," *Lipids* 25 (1990): 48–53, https://doi.org/10.1007/BF02562427.

6. D. K. Park, J. Terao, and S. Matsushita, "Influence of the Positions of Unsaturated Acyl Groups in Glycerides on Autoxidation," *Agricultural and Biological Chemistry* 47, no. 10 (1983): 2251–2255, https://doi.org/10.1080/00021369.1983.10865949.

7. X.-Y. Wang, D. Yang, L.-J. Gan, et al., "Effect of Positional Distribution of Linoleic Acid on Oxidative Stability of Triacylglycerol Molecules Determined by ^{1}H NMR," *Journal of the American Oil Chemists' Society* 92 (2015): 157–165, https://doi.org/10.1007/s11746-015-2590-y.

8. Y. Yamamoto, Y. Imori, and S. Hara, "Oxidation Behavior of Triacylglycerol Containing Conjugated Linolenic Acids in sn-1(3) or sn-2 Position," *Journal of Oleo Science* 63, no. 1 (2014): 31–37, https://doi.org/10.5650/jos.ess13129.

9. Y. Endo, S. Hoshizaki, and K. Fujimoto, "Autoxidation of Synthetic Isomers of Triacylglycerol Containing Eicosapentaenoic Acid," *Journal of the American Oil Chemists' Society* 74, no. 5 (1997): 543–548, https://doi.org/10.1007/s11746-997-0178-x.

10. Y. Endo, S. Hoshizaki, and K. Fujimoto, "Oxidation of Synthetic Triacylglycerols Containing Eicosapentaenoic and Docosahexaenoic Acids: Effect of Oxidation System and Triacylglycerol Structure," *Journal of the American Oil Chemists' Society* 74 (1997): 1041–1045, https://doi.org/10.1007/s11746-997-0022-3.

11. C. Wijesundera, C. Ceccato, P. Watkins, et al., "Docosahexaenoic Acid Is More Stable to Oxidation When Located at the sn-2 Position of Triacylglycerol Compared to sn-1(3)," *Journal of the American Oil Chemists' Society* 85 (2008): 543–548, https://doi.org/10.1007/s11746-008-1224-z.

12. Z. Shen and C. Wijesundera, "Effects of Docosahexaenoic Acid Positional Distribution on the Oxidative Stability of Model Triacylglycerol in Water Emulsion," *Journal of Food Lipids* 16 (2009): 62–71, https://doi.org/10.1111/j.1745-4522.2009.01132.x.

13. A. Damerau, E. Ahonen, M. Kortesniemi, et al., "Docosahexaenoic Acid in Regio- and Enantiopure Triacylglycerols: Oxidative Stability and Influence of Chiral Antioxidant," *Food Chemistry* 402 (2023): 134271, https://doi.org/10.1016/j.foodchem.2022.134271.

14. K. M. Schaich, "Thinking Outside the Classical Chain Reaction Box of Lipid Oxidation," *Lipid Technology* 24, no. 3 (2012): 55–58, https://doi.org/10.1002/lite.201200170.

15. A. Halldorsson, C. D. Magnusson, and G. G. Haraldsson, "Chemoenzymatic Synthesis of Structured Triacylglycerols by Highly Regioselective Acylation," *Tetrahedron* 59, no. 46 (2003): 9101–9109, https://doi.org/10.1016/j.tet.2003.09.059.

16. B. Kristinsson and G. G. Haraldsson, "Chemoenzymatic Synthesis of Enantiopure Structured Triacylglycerols," *Synlett* 14 (2008): 2178–2182, https://doi.org/10.1055/s-2008-1077981.

17. C. D. Magnusson and G. G. Haraldsson, "Chemoenzymatic Synthesis of Symmetrically Structured Triacylglycerols Possessing Short-Chain Fatty Acids," *Tetrahedron* 66, no. 14 (2010): 2728–2731, https://doi.org/10.1016/j.tet.2010.01.110.

18. B. Kristinsson, K. M. Linderborg, H. Kallio, and G. G. Haraldsson, "Synthesis of Enantiopure Structured Triacylglycerols," *Tetrahedron: Asymmetry* 25, no. 2 (2014): 25–132, https://doi.org/10.1016/j.tetasy.2013.11.015.

19. M. Kalpio, J. D. Magnússon, H. G. Gudmundsson, et al., "Synthesis and Enantiospecific Analysis of Enantiostructured Triacylglycerols Containing n-3 Polyunsaturated Fatty Acids," *Chemistry and Physics of Lipids* 231 (2020): 104937, https://doi.org/10.1016/j.chemphyslip.2020.104937.

20. E. Ahonen, A. Damerau, J.-P. Suomela, M. Kortesniemi, and K. M. Linderborg, "Oxidative Stability, Oxidation Pattern and α-tocopherol Response of Docosahexaenoic Acid (DHA, 22:6*n*–3)-Containing Triacylglycerols and Ethyl Esters," *Food Chemistry* 387 (2022): 132882, https://doi.org/10.1016/j.foodchem.2022.132882.

21. W. W. Christie and X. Han, *Lipid Analysis. Isolation, Separation, Identification and Lipidomic Analysis*, 4th ed. (The Oily Press, 2010).

22. H. Tsugawa, T. Cajka, T. Kind, et al., "MS-DIAL: Data-Independent MS/MS Deconvolution for Comprehensive Metabolome Analysis," *Nature Methods* 12 (2015): 523–526, https://doi.org/10.1038/nmeth.3393.

23. A. Damerau, E. Ahonen, M. Kortesniemi, A. Puganen, M. Tarvainen, and K. M. Linderborg, "Evaluation of the Composition and Oxidative Status of Omega-3 Fatty Acid Supplements on the Finnish Market Using NMR and SPME—GC–MS in Comparison With Conventional Methods," *Food Chemistry* 330 (2020): 127194, https://doi.org/10.1016/j.foodchem.2020.127194.

24. D. W. H. Merkx, G. T. S. Hong, A. Ermacora, and J. P. M. van Duynhoven, "Rapid Quantitative Profiling of Lipid Oxidation Products in a Food Emulsion by ^{1}H NMR," *Analytical Chemistry* 90, no. 7 (2018): 4863–4870, https://doi.org/10.1021/acs.analchem.8b00380.

25. G. Beltrame, E. Ahonen, A. Damerau, H. G. Gudmundsson, G. G. Haraldsson, and K. M. Linderborg, "Lipid Structure Influences the Digestion and Oxidation Behavior of Docosahexaenoic and Eicosapentaenoic Acids in the Simulated Digestion System," *Journal of Agricultural and Food Chemistry* 71, no. 26 (2023): 10087–10096, https://doi.org/10.1021/acs.jafc.3c02207.

26. S. D. Segall, W. E. Artz, D. S. Raslan, V. P. Ferraz, and J. A. Takahashi, "Triacylglycerol Analysis of Pequi (*Caryocar brasiliensis* Camb.) Oil by Electrospray and Tandem Mass Spectrometry," *Journal of the Science of Food and Agriculture* 86, no. 3 (2006): 445–452, https://doi.org/10.1002/jsfa.2349.

27. E. N. Frankel, "Volatile Lipid Oxidation Products," *Progress in Lipid Research* 22, no. 1 (1982): 1–33, https://doi.org/10.1016/0163-7827(83)90002-4.

28. E. Ahonen, A. Damerau, and K. M. Linderborg, "Antioxidative Effect of Dihydrosphingosine (d18:0) and α-Tocopherol on Tridocosahexaenoin (DHA-TAG)," *Journal of Agricultural and Food Chemistry* 71, no. 40 (2023): 14769–14781, https://doi.org/10.1021/acs.jafc.3c02668.

29. A. Martínez-Yusta, E. Goicoechea, and M. D. Guillén, "A Review of Thermo-Oxidative Degradation of Food Lipids Studied by ^{1}H NMR Spectroscopy: Influence of Degradative Conditions and Food Lipid Nature," *Comprehensive Reviews in Food Science and Food Safety* 13, no. 5 (2014): 838–859, https://doi.org/10.1111/1541-4337.12090.

30. K. M. Schaich, "Lipid Oxidation: Theoretical Aspects," in *Bailey's Industrial Oil and Fat Products*, ed. F. Shahidi (John Wiley & Sons, Inc, 2005), 269–355.

31. K. G. Raghuveer and E. G. Hammond, "The Influence of Glyceride Structure on the Rate of Autoxidation," *Journal of the American Oil Chemists' Society* 44, no. 4 (1967): 239–243, https://doi.org/10.1007/BF02639266.

Supporting Information

Additional supporting information can be found online in the Supporting Information section.